Available online at www.sciencedirect.com
ScienceDirect
Trans. Nonferrous Met. Soc. China 23(2013) 3456−3461
Transactions of Nonferrous Metals Society of China
www.tnmsc.cn

Thermodynamics analysis of Ni^{2+}−$C_2H_8N_2$−$C_2O_4^{2-}$−H_2O system and preparation of Ni microfiber

Yong-lin YAO, Chuan-fu ZHANG, Jing ZHAN, Feng-hua DING, Jian-hui WU

School of Metallurgy and Environment, Central South University, Changsha 410083, China

Received 27 March 2013; accepted 18 June 2013

Abstract: According to the principles of simultaneous equilibrium and mass equilibrium, the thermodynamics model of the precipitation-coordination equilibrium of Ni^{2+}−$C_2H_8N_2$−$C_2O_4^{2-}$−H_2O system was established, and calculation for the relationships between concentration of each substance in solution and parameters was carried out, including pH value, concentrations of ethylenediamine and oxalate by MATLAB program. The results show that Ni exists as Ni^{2+} and $[Ni(C_2O_4)_n]^{2-2n}$ mainly at pH<1 and pH=1−6, respectively. When pH> 6, the complex between Ni^{2+} and ethylenediamine is predominant. The precursor of Ni microfiber was prepared by an oxalate precipitation process using ethylenediamine as a coordination agent, and the role of ethylenediamine in the growth of the precursor fiber was discussed. The Ni microfiber can be obtained by a thermal decomposition-reduction process of the precursor in N_2 and H_2 mixed atmosphere. The diameters and aspect ratios of the obtained Ni microfibers are 0.2−1 μm and 20−30, respectively.

Key words: thermodynamics analysis; Ni microfiber; precursor; thermal decomposition; reduction

1 Introduction

As an important transition metal material, superfine nickel powder has some unique properties in electromagnetism, heat, light and chemical activity areas because of its super volume effect, surface effect, and good thermal and electrical conductivity [1,2]. Micro- and nano-nickel powders are widely used as catalyst [3−5], electronical slurry [6], microwave absorbing material [7] and so on. Up to date, some methods including carbonyl process [8], liquid reduction method [9] and mechanochemical method [10] are widely used for preparation of superfine nickel powder; however, the carbonyl process is toxic, and the shape is difficult to control by liquid reduction and mechanochemistry method.

The shape of a material has a great influence on its property. Magnetic metal fiber is a potential microwave absorbing material because of its unique shape anisotropy. The polycrystal iron fiber including Fe, Co, Ni and their alloy fibers as microwave absorbing materials were researched by many people [11−13]. Template-based approaches are widely used for the preparation of magnetic metal micro/nano fibers and wires. Many magnetic metal fibers/wires were successfully synthesized by porous anodic aluminum oxide (AAO) or polycarbonate membrane as template [14,15]. However, this method has a complicated process and a low yield which limit its wide application. The precursor of nickel microfiber can be prepared by an oxalate coordination precipitation method with ammonia as a coordination agent, and the nickel fiber can be obtained by a thermal decomposition-reduction process for the precursor [16−18]. But the pH value of the Ni^{2+}−NH_3−$C_2O_4^{2-}$−H_2O system for obtaining precursor fibers is high (~9), which will lead to an equipment spoilage and environmental pollution. In this work, we prepared a new Ni precursor fiber at a neutral environment (pH=6.5) and a less dosage of coordination agent with ethylenediamine instead of ammonia as a coordination agent. The precipitation−coordination equilibrium of Ni^{2+}−$C_2H_8N_2$−$C_2O_4^{2-}$−H_2O system was first calculated and the effects of pH, concentrations of ethylenediamine and oxalate on the precipitation process were determined. The role of ethylenediamine in the

Foundation item: Project (CX2012B046) supported by Hunan Provincial Innovation Foundation for Postgraduate, China; Project (20090162120080) supported by the Doctorate Fund of Education Minister of China
Corresponding author: Jing ZHAN; Tel: +86-731-88836048; E-mail: zhanjing2001@hotmail.com
DOI: 10.1016/S1003-6326(13)62888-5

fiber growth mechanism was revealed, which can provide reference for other fiber preparation by coordination precipitation process. The precursor was decomposed and reduced in N_2 and H_2 mixed atmosphere and the nickel fiber can be obtained.

2 Precipitation−coordination equilibrium of Ni^{2+}−$C_2H_8N_2$− $C_2O_4^{2-}$ −H_2O system

2.1 Establishment of precipitation−coordination equilibrium model

$C_2H_8N_2$, $C_2O_4^{2-}$ and OH^- can combine with Ni^{2+} to form complex compounds in the Ni^{2+}−$C_2H_8N_2$− $C_2O_4^{2-}$ −H_2O system, and the accumulation formation constants (β) are listed in Table 1 [19].

Table 1 Cumulative formation constants of complexes

Complex	NiC_2O_4	$Ni(C_2O_4)_2^{2-}$	$Ni(C_2O_4)_3^{4-}$
lg β	5.3	7.64	8.5
Complex	$Ni(C_2H_8N_2)^{2+}$	$Ni(C_2H_8N_2)_2^{2+}$	$Ni(C_2H_8N_2)_3^{2+}$
lg β	7.52	13.84	18.33
Complex	$Ni(OH)^+$	$Ni(OH)_2$	$Ni(OH)_3^-$
lg β	4.97	8.55	11.33

The reaction equilibrium constants (K) of the acid−base equilibrium reaction between oxalate and ethylenediamine are listed in Table 2 [19].

Table 2 Equilibrium constants of oxalate and ethylenediamine

Equation	lg K
$H_2C_2O_4 = HC_2O_4^- + H^+$	−1.271
$HC_2O_4^- = C_2O_4^{2-} + H^+$	−4.272
$(C_2H_{10}N_2)^{2+} = (C_2H_9N_2)^+ + H^+$	−6.85
$(C_2H_9N_2)^+ = C_2H_8N_2 + H^+$	−9.92

$[Ni]_T$, $[C_2O_4]_T$, $[C_2H_8N_2]_T$ and $[OH]_T$ are analytical concentrations of each composition in solution, and according to mass balance and simultaneous equilibrium principle, and we can get some equations as follows:

$$[Ni]_T=[Ni^{2+}]+[Ni(OH)^+]+[Ni(OH)_2]+[Ni(OH)_3^-]+[Ni(C_2O_4)]+[Ni(C_2O_4)_2^{2-}]+[Ni(C_2O_4)_3^{4-}]+[Ni(C_2H_8N_2)^{2+}]+[Ni(C_2H_8O_4)_2^{2+}]+[Ni(C_2H_8O_4)_3^{2+}]$$

$$[C_2O_4]_T=[Ni(C_2O_4)]+2[Ni(C_2O_4)_2^{2-}]+3[Ni(C_2O_4)_3^{4-}]+[(C_2O_4)^{2-}]+[H(C_2O_4)^-]+[H_2(C_2O_4)]$$

$$[C_2H_8N_2]_T=[C_2H_8N_2]+[C_2H_9N_2^+]+[C_2H_{10}N_2^{2+}]+[Ni(C_2H_8N_2)^{2+}]+2[Ni(C_2H_8N_2)_2^{2+}]+3[Ni(C_2H_8N_2)_3^{2+}]$$

$$[OH]_T=[NiOH^+]+2[Ni(OH)_2]+3[Ni(OH)_3^-]+[OH^-]$$

Ni^{2+} can combine with $C_2O_4^{2-}$ or OH^- to form oxalate or hydroxide precipitate at different conditions and the solubilities (K_{sp}) of each precipitate are listed in Table 3 [19].

Table 3 Solubility products of NiC_2O_4 and $Ni(OH)_2$

Equation	lg K_{sp}
$NiC_2O_4(s) = Ni^{2+} + C_2O_4^{2-}$	−9.40
$Ni(OH)_2(s) = Ni^{2+} + 2OH^-$	−14.70

When $NiC_2O_4(s)$ exists in the solution, the concentration of Ni^{2+} can be calculated by $[Ni^{2+}]=K_{sp}/[C_2O_4^{2-}]$. The $NiC_2O_4(s)$ will convert to $Ni(OH)_2(s)$ when pH is high enough and the concentration of Ni^{2+} can be calculated by $[Ni^{2+}]=K_{sp}/[OH^-]^2= K_{sp}\times10^{28-2pH}$. From the above, the concentration of Ni^{2+} can be described as $[Ni^{2+}]=\{10^{-9.4}/[C_2O_4^{2-}], 10^{13.3-2pH}\}_{min}$.

The concentration of each substance in the solution can be calculated using MATLAB program according to the mass equilibrium, complex equilibrium, acid−base equilibrium and precipitate equilibrium equations. Here we only calculated the results at pH<10 to avoid the form of hydroxide precipitate at high pH values.

2.2 Calculation results

Figure 1 shows the relationships of $[Ni]_T$ with pH and $[C_2H_8N_2]_T$ at $[C_2O_4]_T$= 0.1 mol/L. Figure 2 indicates the corresponding distribution state of Ni in solution. As shown in Fig. 1, when pH<1, $NiC_2O_4(s)$ will dissolve to a certain extent. In this case, Ni exists as Ni^{2+} mainly which is confirmed in Fig. 2. With the increase of pH, $[Ni]_T$ decreases because the dissociation of $H_2C_2O_4$ and $HC_2O_4^-$ leads to a rise of $[C_2O_4^{2-}]$ and the precipitation rate of $NiC_2O_4(s)$ increases. When pH=1−6, $C_2O_4^{2-}$ will combine with Ni^{2+} and $[Ni(C_2O_4)_n]^{2-2n}$ is the main existing form of Ni according to Fig. 2, and so the change law of Ni^{2+} precipitation rate with pH is similar with that of $[Ni(C_2O_4)_n]_T^{2-2n}$. When pH>6, the complex

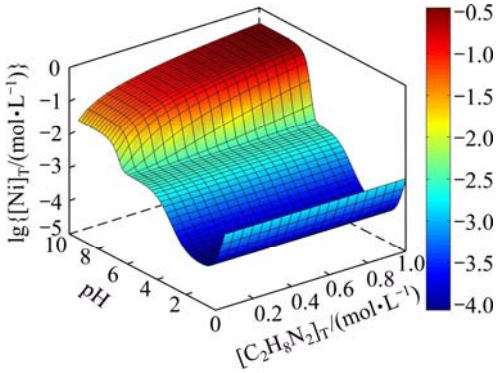

Fig. 1 Relationships among $[Ni]_T$ and pH and $[C_2H_8N_2]_T$ at $[C_2O_4]_T$= 0.1 mol/L

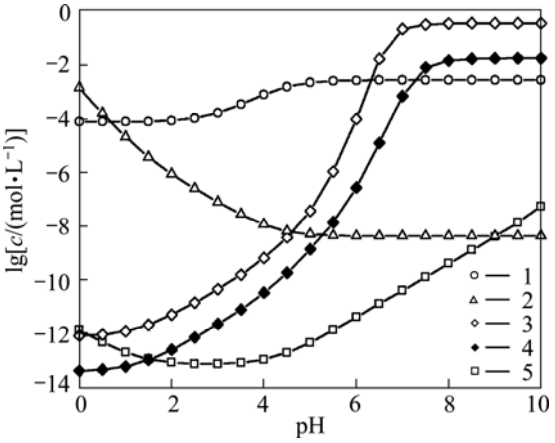

Fig. 2 Relationships between each Ni species and pH at $[C_2O_4]_T$= 0.1 mol/L: 1—$[Ni(C_2O_4)_n]_T^{2-2n}$ at $[C_2H_8N_2]_T$= 0.1−1.0 mol/L; 2—$[Ni^{2+}]$ at $[C_2H_8N_2]_T$ = 0.1−1.0 mol/L; 3—$[Ni(C_2H_8N_2)_n]_T^{2+}$, at $[C_2H_8N_2]_T$ = 1.0 mol/L; 4—$[Ni(C_2H_8N_2)_n]_T^{2+}$, at $[C_2H_8N_2]_T$ = 0.1 mol/L; 5—$[Ni(OH)_n]_T^{2-n}$ at $[C_2H_8N_2]_T$= 0.1−1.0 mol/L

between ethylenediamine and Ni^{2+} is superior, which leads to a further decrease of the precipitation rate. As shown in Fig. 2, the concentration of ethylenediamine does not influence the concentrations of Ni^{2+}, $[Ni(C_2O_4)_n]^{2-2n}$ and $[Ni(OH)_n]^{2-n}$, but is positively correlated with the concentration of $[Ni(C_2H_8N_2)_n]_T^{2+}$. So, the precipitation rate changes hardly with the variation of ethylenediamine at pH<6 but decreases with the increase of the concentration of ethylenediamine at pH>6.

Figure 3 shows the relationships of $[Ni]_T$ with pH and $[C_2O_4]_T$ at $[C_2H_8N_2]_T$=0.1 mol/L. Figure 4 indicates the corresponding distribution state of Ni in solution. When pH<1, $[Ni]_T$ decreases with the increase of $[C_2O_4]_T$. Associating with Fig. 4, the concentration of $[Ni(C_2O_4)_n]^{2-2n}$ has little relationship with $[C_2O_4]_T$ in the range of pH< 1, which indicates that the precipitation action rather than the complex between $C_2O_4^{2-}$ and Ni^{2+} is predominant. When pH=1−6, it can be seen that

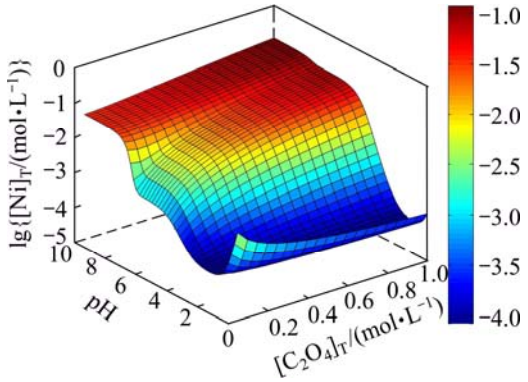

Fig. 3 Relationships among $[Ni]_T$ and pH and $[C_2O_4]_T$ at $[C_2H_8N_2]_T$= 0.1 mol/L

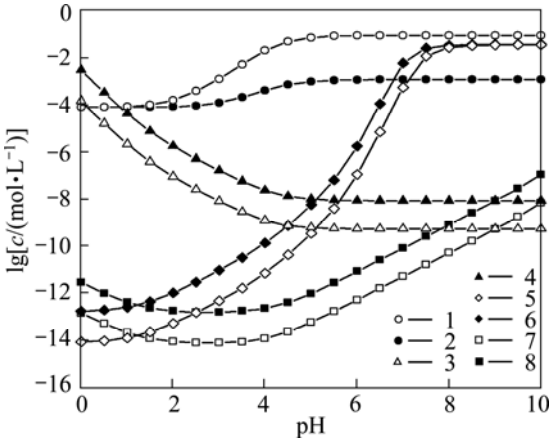

Fig. 4 Relationships between each Ni species and pH at $[C_2H_8N_2]_T$=0.1 mol/L: 1—$[Ni(C_2O_4)_n]_T^{2-2n}$ at $[C_2O_4]_T$= 1.0 mol/L; 2—$[Ni(C_2O_4)_n]_T^{2-2n}$ at $[C_2O_4]_T$=0.1 mol/L; 3—Ni^{2+} at $[C_2O_4]_T$=1.0 mol/L; 4—Ni^{2+} at $[C_2O_4]_T$=0.1 mol/L; 5—$[Ni(C_2H_8N_2)_n]_T^{2+}$ at $[C_2O_4]_T$=1.0mol/L; 6—$[Ni(C_2H_8N_2)_n]_T^{2+}$ at $[C_2O_4]_T$=0.1 mol/L; 7—$[Ni(OH)_n]_T^{2-n}$ at $[C_2O_4]_T$=1.0 mol/L; 8—$[Ni(OH)_n]_T^{2-n}$ at $[C_2O_4]_T$=0.1 mol/L

Ni exists as $[Ni(C_2O_4)_n]^{2-2n}$ mainly and $[Ni(C_2O_4)_n]_T^{2-2n}$ will increase with the increase of $[C_2O_4]_T$, which leads to the same change trend for $[Ni]_T$ shown in Fig. 3. When pH>6, $Ni(C_2O_4)_n]_T^{2-2n}$ has little change and the complex between Ni^{2+} and ethylenediamine determines the precipitation rate.

It is noted that the system of Ni^{2+}−$C_2H_8N_2$−$C_2O_4^{2-}$−H_2O is complicated and the analyses above are the results in certain conditions (such as $[C_2O_4]_T$=0.1 mol/L, $[C_2H_8N_2]_T$=0.1 mol/L). But we can get the results in any condition with the above method because of the same principle. The change laws of precipitation rate and each Ni species with pH have a guiding significance for the preparation of Ni precursor fiber, which is discussed in detail in the next section.

3 Preparation of Ni microfiber

3.1 Experimental

All the reagents including $H_2C_2O_4·2H_2O$, $NiCl·6H_2O$, ethylenediamine, and ethanol are analytically pure. The $H_2C_2O_4$ and $NiCl_2$ solutions with a certain concentration were prepared and their pH values were adjusted by ethylenediamine. The two solutions were mixed and stirred at 60 °C for 3 h and some blue precipitates (precursors) can be obtained. The precursors were washed with ethanol and water three times and then dried at 60 °C for 4 h. The dried precursors were decomposed and reduced in N_2 and H_2 mixed atmosphere $V(N_2):V(H_2)$=9:1 at 420 °C for 30 min and the nickel microfibers can be obtained. X-ray diffraction

(XRD, TTR III) was applied to determining the phase compositions of precursors and Ni microfibers. The morphologies of the precursors and Ni microfibers were observed with an electron scanning microscope (SEM, JSM−6360LV) and the composition of the Ni microfibers was characterized with the energy dispersive spectrometer (EDS, GENESIS) equipped on the SEM.

3.2 Results and discussion

Figures 5 (a) and (b) show the XRD patterns of precursors prepared at pH<2 (no addition of ethylenediamine) and pH=6.5, respectively. As shown in Fig. 5(a), in the case of no ethylenediamine addition, the crystal structure of precursor can be determined as $NiC_2O_4{\cdot}2H_2O$ according to the Joint Committee on Powder Diffraction Standards (JCPDS, No. 25—0581). However, there is no corresponding JCPDS card with the precursor prepared at pH=6.5. For $Ni^{2+}-C_2O_4^{2-}-C_2H_8N_2$ system, the coordination of Ni and $C_2H_8N_2$ can be described as $[Ni(C_2H_8N_2)(C_2O_4)]$ chains [20], and single crystal of $Ni(C_2H_8N_2)(C_2O_4){\cdot}2H_2O$ has been synthesized [21]. So, we suppose that during the precipitation process, the ethylenediamine combined Ni ions and formed a new crystal structure which can be described as $[Ni(C_2H_8N_2)_y]C_2O_4{\cdot}xH_2O$ [22] and the exact structural formula will be determined in a further study.

The SEM photographs of precursors prepared at different pH values are shown in Fig. 6. When no ethylenediamine is added, the precursors are clusters consisting of some cube particles. Under this circumstance, the direct contact of oxalate and Ni^{2+} causes a quick nucleation and many crystal nucleus bump and form an agglomeration. When ethylenediamine is added, Ni^{2+} will combine with it and the speed of nucleation and growth can be controlled, which is beneficial to obtaining separated particles, as shown in Fig. 6(b). When the concentration of ethylenediamine increases to a certain extent (pH=6), the growth pattern of precursor changes and the fibrous precursors appear, but the shape is not uniform and some breakages and branches exist. When pH=6.5, the shapes of precursors become uniform and the surfaces are smooth.

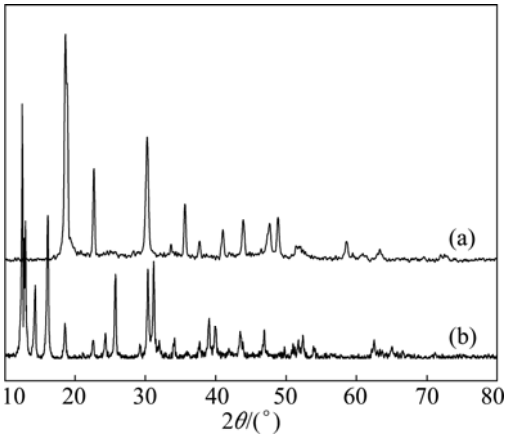

Fig. 5 XRD patterns of precursors prepared at pH<2 (no addition of ethylenediamine, $NiC_2O_4{\cdot}2H_2O$) (a) and pH=6.5 (b)

According to the above equilibrium calculation results, the pH value should be controlled at 1−3 for a

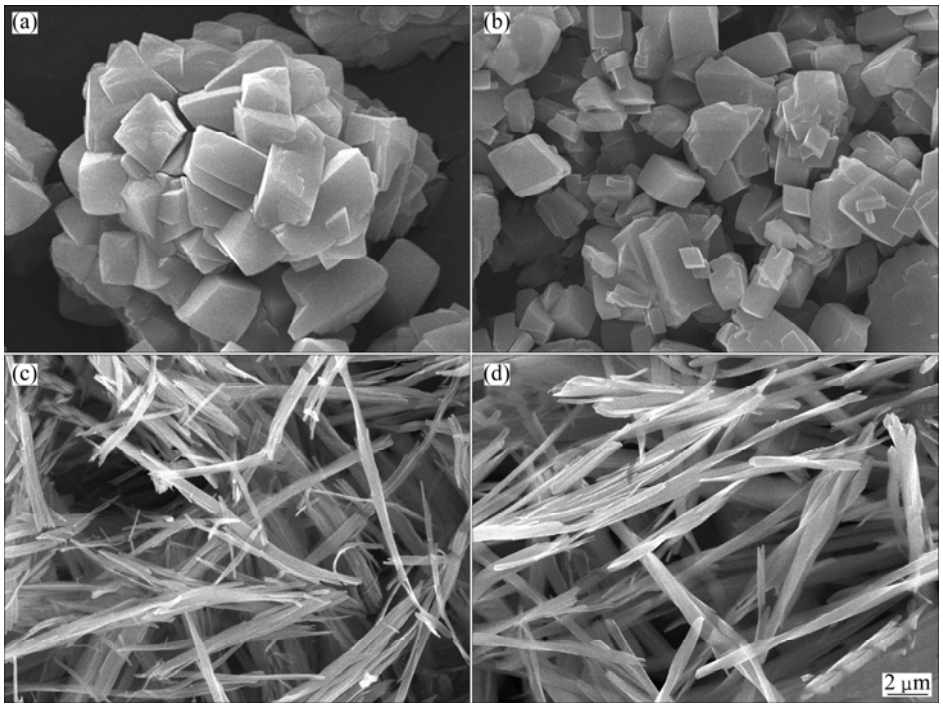

Fig. 6 SEM images of precursors prepared at different pH values: (a) Without ethylenediamine (pH<2); (b) pH=5.5; (c) pH=6.0; (d) pH=6.5

satisfactory precipitation rate. However, the pH value has an important effect on the precursor shape. The complex of ethylenediamine and Ni^{2+} is not dominant at pH<6 but it becomes superior at pH>6. This corresponds to the shape change process in which the precursor is cube-like and fiber-like at pH<6 and pH>6, respectively. In our experiment, the addition of ethylenediamine was controlled by pH, so we can conclude that ethylenediamine can change the growth pattern of precursor. Micron-sized precipitated powder is usually an agglomerate of small crystallites and the crystallites aggregate to a certain shape under the action of surface energy differences [23]. In the precipitation process, ethylenediamine can be adsorbed on a certain crystal face of the precursor and restrain its growth due to the surface energy change, which causes the final formation of fibrous precursor. The result is consistent with the phenomenon in other coordinated-precipitation process using ammonia as coordination agent [24,25]. But when pH>7, the complex of ethylenediamine and Ni^{2+} becomes serious, which may cause a bad precipitation rate even the precursor precipitate cannot be obtained, so giving consideration to both precipitation rate and precursor shape, the pH should be controlled at 6.5.

Figure 7 shows the XRD pattern of the Ni microfibers through thermal decomposition−reduction of precursor fibers. As shown in Fig. 7, the sample shows a good crystallinity and the peaks match well with those of the JCPDS (No. 04—0850) data of Ni. The XRD pattern without impurity peaks indicates that the product has a high purity.

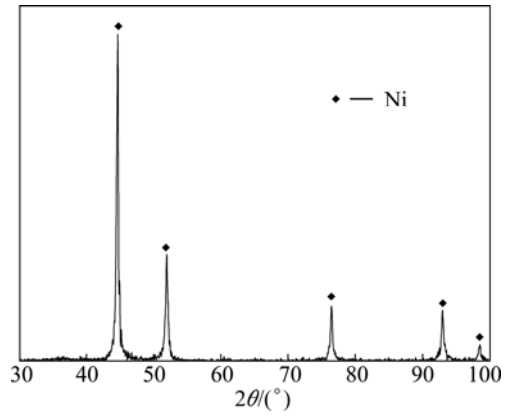

Fig. 7 XRD pattern of Ni microfibers

Figure 8(a) shows the SEM image of the Ni microfibers from which we can see the diameters of the fibers are 0.2−1 μm, and the aspect ratios are 20−30. The surfaces are not smooth as the precursors because of the release of CO, CO_2 and ethylenediamine in the thermal decomposition process. As shown in Fig. 8(b), the EDS spectrum further indicates the purity of the Ni microfibers.

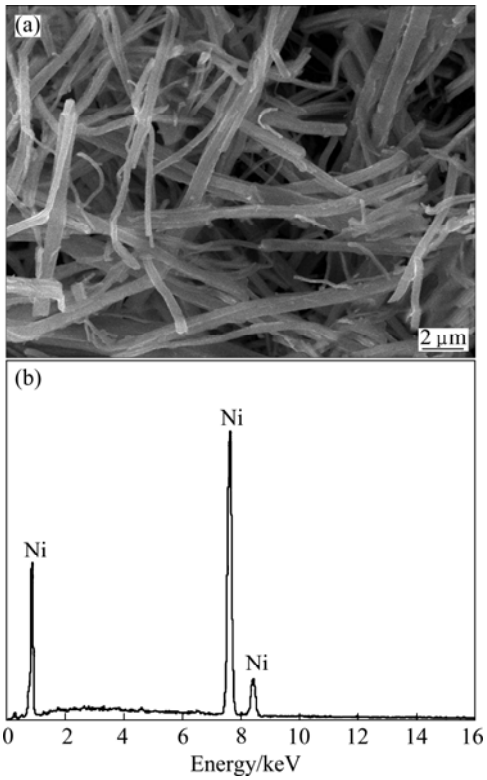

Fig. 8 SEM image (a) and EDS spectrum (b) of Ni microfibers

4 Conclusions

1) The precipitation−coordination equilibrium model of Ni^{2+}–$C_2H_8N_2$– $C_2O_4^{2-}$ –H_2O system was established and calculated by MATLAB program. Ni exists as Ni^{2+} and $[Ni(C_2O_4)_n]^{2-2n}$ mainly at pH<1 and pH=1−6, respectively. When pH>6, the complex between Ni^{2+} and ethylenediamine is predominant. All substances except $[Ni(C_2O_4)_n]_T^{2-2n}$ are positively correlated with $[C_2O_4]_T$ but only $[Ni(C_2H_8N_2)_n]_T^{2+}$ increases with the increase of $[C_2H_8N_2]_T$.

2) The Ni precursor fiber was prepared at pH=6.5 by an oxalate precipitation process with ethylenediamine as a coordination agent, and the growth mechanism can be changed with the addition of ethylenediamine. The pure Ni microfiber can be obtained by a thermal decomposition-reduction of the precursor fiber at 420 °C for 30 min in N_2 and H_2 mixed atmosphere. The diameters and aspect ratios of the obtained Ni microfiber are 0.2−1 μm and 20−30, respectively.

References

[1] SANCAKTAR E, DILSIZ N. Pressure dependent conduction behavior of various particles for conductive adhesive applications [J]. Journal of Adhesion Science and Technology, 1999, 13(6): 679−693.

[2] CHEN Li-bao, HE Yue-hui, DENG Yi-da. Present status and development trend of nickel and cobalt powder [J]. Powder Metallurgy Technology, 2004, 22(3): 173−177. (in Chinese)

[3] KAPOO S, SALUNKE H G, TRIPATHI A K, KULSHRESHTHA S K, MITTAL J P. Radiolytic preparation and catalytic properties of nanophase nickel particles [J]. Materials Research Bulletion, 2000, 35(1): 143−148.
[4] TENG C C, KU F C, SUNG C M, DENG J P, CHIEN S F, SONG S M, LIN C T. Effect of nano-Ni catalyst on the growth and characterization of diamond films by HFCVD [J]. Journal of Nanomaterials, 2010, 2010: 365614.
[5] CAO Chang-yan, CHEN Chao-qiu, LI Wei, SONG Wei-guo, CAI Wei. Nanoporous nickel spheres as highly active catalyst for hydrogen generation from ammonia borane [J]. Chem Sus Chem, 2010, 3(11): 1241−1244.
[6] WANG Sen, ZHANG Yue, JI Zhen, LI Ling-feng, ZHOU Cheng. Investigation on the rheological behavior of Ni-contained electronical slurry [J]. Journal of Functional Materials, 2005, 36(6): 869−871. (in Chinese)
[7] LIU T, ZHOU P H, XIE J L, DENG L J. Electromagnetic and absorption properties of urchinlike Ni composites at microwave frequencies [J]. Journal of Applied Physics, 2012, 111(9): 093905.
[8] IWAI K, YASUDA H. Carbonyl nickel powder [J]. New Materials & New Processes, 1985, 3: 241−244.
[9] LI Y D, LI C W, WANG H R, LI L Q, QIAN Y T. Preparation of nickel ultrafine powder and crystalline film by chemical control reduction [J]. Materials Chemistry and Physics, 1999, 59(1): 88−90.
[10] BABURAJ E G, KEVIN T, HUBERT F H. Preparation of Ni powder by mechanochemical process [J]. Journal of Alloys and Compounds, 1997, 257(1−2): 146−149.
[11] QIAO Liang, HAN Xiang-hua, GAO Bo, WANG Jian-bo, WEN Fu-sheng. Microwave absorption properties of the hierarchically branched Ni nanowire composites [J]. Journal of Applied Physics, 2009, 105(5): 053911.
[12] YU Ming-xun, LI Xiang-cheng, GONG Rong-zhou, HE Yan-fei, HE Hua-hui, LU Pei-xiang. Magnetic properties of carbonyl iron fibers and their microwave absorbing characterization as the filer in polymer foams [J]. Journal of Alloys and Compounds, 2008, 456(1−2): 452−455.
[13] YI J W, LEE S B, KIM J B, LEE S K, KIM K H, PARK O O. Evaluation of composites containing hollow Ni/Fe−Co fibers on near-field electromagnetic wave absorbing properties [J]. Advanced Materials Research, 2010, 123−125: 1223−1226.
[14] ALMASI KASHI M, RAMAZANI A, DOUDAFKAN S, ESMAEILY A S. Microstructure and magnetic properties in arrays of ac electrodeposited Fe_xNi_{1-x} nanowires induced by the continuous and pulse electrodeposition [J]. Applied Physics A, 2011, 102(3): 761−764.
[15] XUE Shou-hong, LI Mei, WANG You-hong, XU Xi-min. Electrochemically synthesized binary alloy FeNi nanorod and nanotube arrays in polycarbonate membranes [J]. Thin Solid Films, 2009, 517(20): 5922−5926.
[16] ZHANG Chuan-fu, WU Jian-hui, ZHAN Jing, LI Chang-jun, DAI Xi. Precursor synthesis of fibrillar nanocrystalline nickel powder [J]. Nonferrous Metals, 2003, 55(3): 25−29. (in Chinese)
[17] LI Tao, LIU Ying, PENG Tong-jiang, MA Guo-hua, YANG Xiao-jiao. Controlled synthesis of polycrystalline nickel oxalate nanofibers by the mild thermal precipitation and aging process [J]. Journal of Wuhan University of Technology: Materials Science Edition, 2011, 26(6): 1041−1043.
[18] OKAMOTO T, ICHINO R, OKIDO M, LIU Zhi-hong, ZHANG Chuan-fu. Effect of ammonia on the crystal morphology of nickel oxalate precipitates and their thermal decomposition into metallic nickel [J]. Materials Transactions, 2005, 48(2): 171−174.
[19] DEAN J A. Lange's handbook of chemistry [M]. SHANG Jiu-fang, et al transl. Beijing: Science, 1991. (in Chinese)
[20] KITAGAWA S, OKUBO T, KAWATA S, KONDO M, KATADA M, KOBAYASHI H. An oxalate-linked copper (II) coordination polymer, $[Cu_2(oxalate)_2(pyrazine)_3]_n$, constructed with two different copper units: X-ray crystallographic and electronic structures[J]. Inorganic Chemistry, 1995, 34(19): 4790−4796.
[21] CHUN J, LEE Y, PYO S, IM C, KIM S, YUN H, DO J. Synthesis, structure, and magnetic properties of 1D nickel coordination polymer $Ni(en)(ox)\cdot 2H_2O$ (en= ethylenediamine; ox= oxalate) [J]. Bulletin of the Korean Chemical Society, 2009, 30(7): 1603−1606.
[22] ZHANG Chuan-fu, YAO Yong-lin, ZHANG Yin-liang, ZHAN Jing. Preparation of ultra-fine fibrous Fe−Ni alloy powder by coordinated co-precipitation-direct reduction process [J]. Transactions of Nonferrous Metals Society of China, 2012, 22(12): 2972−2978.
[23] JONGEN N, BOWEN P, LEMAITRE J, VALMALETTE J C, HOFMANN H. Precipitation of self-organized copper oxalate polycrystalline particles in the presence of hydroxypropylmethylcellulose (HPMC): Control of morphology [J]. Journal of Colloid and Interface Science, 2000, 226: 189−198.
[24] ZHAN Jing, HE Yue-hui, ZHOU Di-fei, ZHANG Chuan-fu. Thermodynamic analysis on synthesis of fibrous Ni−Co alloys precursor and Ni/Co ratio control [J]. Transactions of Nonferrous Metals Society of China, 2011, 21(5): 1141−1148.
[25] ZHAN Jing, ZHOU Di-fei, ZHANG Chuan-fu. Shape-controlled synthesis of novel precursor for fibrous Ni−Co alloy powders [J]. Transactions of Nonferrous Metals Society of China, 2011, 21(3): 544−551.

$Ni^{2+}-C_2H_8N_2-C_2O_4^{2-}-H_2O$ 体系的热力学分析及 Ni 微米纤维的制备

姚永林，张传福，湛 菁，丁风华，邬建辉

中南大学 冶金与环境学院，长沙 410083

摘 要：根据同时平衡和质量平衡原理，建立了 $Ni^{2+}-C_2H_8N_2-C_2O_4^{2-}-H_2O$ 体系的沉淀−配合平衡热力学模型，并对该模型进行计算来揭示该体系中各物种浓度随 pH 值、草酸及乙二胺浓度的变化规律。结果表明，当 pH<1 和 pH=1−6 时，溶液中的 Ni 分别主要以游离 Ni^{2+}及$[Ni(C_2O_4)_n]^{2-2n}$形式存在。当 pH>6 时，Ni^{2+}与乙二胺的配合作用占优势。当用乙二胺作配位剂，采用草酸盐沉淀法制备了 Ni 微米纤维前驱体，并讨论了乙二胺在前驱体生长机制中的作用。将前驱体在 N_2 和 H_2 混合气氛中热分解还原，可得到直径 0.2~1 μm、长径比 20~30 的 Ni 微米纤维。

关键词：热力学分析；Ni 微米纤维；前驱体；热分解；还原

(Edited by Hua YANG)